On the structural identifiability of joint parameters from motion capture data

Quang-Cuong Pham, Ko Ayusawa, Kanade Kubota, Yoshihiko Nakamura
Department of Mechano-Informatics
University of Tokyo, Japan

***Abstract*—To identify the joint parameters (e.g. the position of the joint center for a spherical joint, the position and the orientation of the joint axis for a revolute joint, etc.) from motion capture data, existing provably-correct algorithms require that at least three markers be attached to either of the two links adjacent to the joint. However, as shown in this article, it turns out that the identification of the joint parameters requires, for most types of joints, strictly less than three markers on any link. More precisely, we prove the structural identifiability of joint parameters in the following cases: (a) a spherical joint with two markers attached to each of the two adjacent links; (b) a revolute joint with two markers attached to one of the two links, and one marker attached to the other. We provide a practical algorithm to do the identification in case (a). Finally, we show that identification cannot be achieved with strictly fewer markers than listed in (a) and (b).**

I. Introduction

Recent applications of motion capture technology, such as musculo-skeletal modeling (see e.g. [7] and references therein) or computer animation (see e.g. [8] and references therein), require the mapping of motion capture data (usually the 3D positions of optical markers) onto an animated skeletal model of the captured subject. A skeletal model usually consists of a certain number of rigid links connected to each other by mechanical joints: e.g. the hip, which connects the trunk and the thigh in the manner of a spherical – or ball – joint, or the knee, which connects the thigh and the shank in the manner of a revolute – or hinge – joint. Since usually the markers cannot be attached directly to the critical locations on the joint (the joint center in a spherical joint, the joint axis in a revolute joint, etc.), an essential task in motion capture analysis consists of determining the joint parameters *indirectly* from the recorded positions of the markers attached to its adjacent links.

In the case of spherical joints, if one link is held stationary or if three markers are attached to one of the two adjacent links, efficient algorithms (see a review in [2]) have been proposed to determine the position of the joint centers. However, in many applications, the links are non-stationary and the total number of markers is limited – sometimes to as few as 16 markers in a full-body setting – making the aforementioned algorithms inapplicable. One way to overcome this difficulty consists of hand-adjusting the positions of the joint centers, but this method is time-consuming and provides no guarantee as for the correctness of the so-determined positions. Other methods consist of solving a very large nonlinear optimization problem [6], but such methods typically suffer from the problem of local minima and usually involve extra penalty costs (e.g. the distance penalty in [6], solely intended to guarantee the convergence of the algorithm to sensible values).

In fact, as shown in this article, the identification of joint parameters requires *strictly less than three markers on any link*. More precisely, we propose to prove the *structural identifiability* [1] of the joint parameters in the following cases: (a) a spherical joint with two markers attached to each of the adjacent links; (b) a revolute joint with two markers attached to one of the two links, and one marker attached to the other. By structural identifiability, we mean that the joints and links are supposed to be strictly rigid (the distance of a marker to the joint center or axis is strictly constant) and that there is no measurement noise. Structural identifiability is a *necessary* condition for actual identifiability: if a system is non structurally identifiable, then *no* algorithm can achieve reliable identification in practice. Note however that the converse is not true in general. Here, in addition to the structural identifiability results, we also present a *practical* algorithm to achieve reliable identification in case (a) and compare the performance of this algorithm with those of existing algorithms [2, 3, 6]. Finally, we show that structural identification cannot be achieved with strictly fewer markers than listed in (a) and (b), establishing thereby the *minimum* numbers of markers required for parameter identification of spherical and revolute joints.

II. Geometric relations between two rigid links

A. General considerations

Consider two rigid links $\mathscr{A}$ and $\mathscr{B}$, which are connected together by a joint (prismatic, revolute, spherical, etc.), whose position and orientation, both in space and with respect to $\mathscr{A}$ and $\mathscr{B}$, are unknown. A certain number of markers are attached to each link, say p markers $A_1, \dots, A_p$ on $\mathscr{A}$ and q markers $B_1, \dots, B_q$ on $\mathscr{B}$. Without loss of generality, we can suppose $p \geq q$ and subsequently place ourselves in a reference frame $\mathcal{F}$ where the p markers of $\mathscr{A}$ are fixed. Remark that, if $p \geq 3$, link $\mathscr{A}$ is fixed in $\mathcal{F}$, whereas, if $p = 2$, the position and orientation of $\mathscr{A}$ is only determined up to a rotation around the axis formed by the two markers at hand.

Let us next denote the coordinates of $B_1, \dots, B_q$ in $\mathcal{F}$ by $\Omega = (x_1, y_1, z_1, \dots, x_q, y_q, z_q)$, which we call the *output* of the system. The set of all possible outputs corresponding to all possible values of the joint is denoted by $\mathcal{S}$. For each frame i of the motion capture data, we thus have one *sample* output

$\Omega^{(i)} = (x_1^{(i)}, y_1^{(i)}, z_1^{(i)}, \dots x_q^{(i)}, y_q^{(i)}, z_q^{(i)}) \in \mathcal{S}$. A N-tuple of samples is called a N-sample, which is an element of $\mathcal{S}^N$.

Let Π denote a tuple of (unknown) parameters that describes the position and orientation of the joint in $\mathcal{F}$. For instance, for a spherical joint, Π can be the Cartesian coordinates (x_J, y_J, z_J) or the cylindrical coordinates (d, r, θ) of the joint center J in $\mathcal{F}$ (see Fig. 1). Following the remark of the previous paragraph, if $p \geq 3$, then (x_J, y_J, z_J) or (d, r, θ) are constant across the frames. By contrast, if $p = 2$, then (x_J, y_J, z_J) and (d, r, θ) are *not* constant. More precisely, if the axis of the cylindrical coordinate system coincides with the axis formed by the two markers of $\mathscr{A}$, then (d, r) are constant across the frames and θ is variable. We then denote by Π_c the tuple of *constant* parameters and Π_v the tuples of *variable* parameters. Similarly, we denote by Σ_c, Σ_v the tuples of (unknown) constant and variable parameters that describe the positions and orientations of $B_1 \dots B_q$ with respect to the joint. For instance, again in the case of spherical joint and $q = 1$, Σ_c can consist of the distance ρ between the joint to the marker and Σ_v can consist of the azimuth and inclination angles (ϕ, ψ) (see Fig. 1).

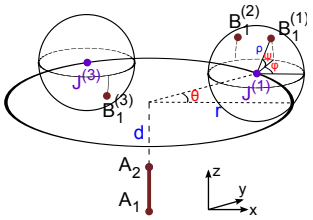

Fig. 1. Example of a spherical joint J connecting two rigid links. Two markers A_1, A_2 are attached to link $\mathscr{A}$ and one marker B_1 is attached to link $\mathscr{B}$. Note that the constant parameters (d, r, ρ), in blue, are the same for all samples $B_1^{(i)}$, whereas the variable parameters (θ, ϕ, ψ), in red, change for each $B_1^{(i)}$.

Finally, let f be the function that relates these parameters to the output as follows

$$\Omega = f(\Pi_c, \Pi_v, \Sigma_c, \Sigma_v).$$

Note that this function f can be computed beforehand for each type of joint. For instance, again in the case of a spherical joint and $p = 2$, $q = 1$, we have $\Omega = (x_1, y_1, z_1)$, $\Pi_c = (d, r)$, $\Pi_v = \theta$, $\Sigma_c = \rho$, $\Sigma_v = (\phi, \psi)$ and f is given by

$$\left\{ \begin{array}{lcl} x_1 & = & r\cos\theta + \rho\cos\phi\sin\psi \\ y_1 & = & r\sin\theta + \rho\sin\phi\sin\psi \\ z_1 & = & d + \rho\cos\psi. \end{array} \right.$$

B. Problem definition

Suppose that we have at our disposal a N-sample $(\Omega^{(1)}, \dots, \Omega^{(N)})$. By construction, the *actual* joint parameters $(\Pi_c, \Pi_v^{(1)}, \dots, \Pi_v^{(N)}, \Sigma_c, \Sigma_v^{(1)}, \dots, \Sigma_v^{(N)})$ are solutions of the following system of equations in the unknowns $(X_c, X_v^1, \dots, X_v^N, Y_c, Y_v^1, \dots, Y_v^N)$

$$\left\{ \begin{array}{lcl} \Omega^{(1)} & = & f(X_c, X_v^1, Y, Y_v^1) \\ & \vdots & \\ \Omega^{(N)} & = & f(X_c, X_v^N, Y_c, Y_v^N). \end{array} \right. \quad (1)$$

The goal of the present article – identifying the position and orientation of the joint – can then be formulated through the following questions

1) Is the tuple $(\Pi_c, \Pi_v^{(1)}, \dots, \Pi_v^{(N)})$ *unique*? That is, if $(\Pi_c', \Pi_v'^{(1)}, \dots, \Pi_v'^{(N)}, \Sigma_c', \Sigma_v'^{(1)}, \dots, \Sigma_v'^{(N)})$ is also solution of (1), do we have necessarily $(\Pi_c', \Pi_v'^{(1)}, \dots, \Pi_v'^{(N)}) = (\Pi_c, \Pi_v^{(1)}, \dots, \Pi_v^{(N)})$?
2) If the $(\Pi_c, \Pi_v^{(1)}, \dots, \Pi_v^{(N)})$ is unique, can we determine it from the N-sample at our disposal?

If the answers to the above two questions are positive, then we say that the N-sample at our disposal is *identifying*. In the opposite case, we say that the N-sample is *non-identifying*. We can now state the following definition of identifiability

Definition 1 We say that the case (p, q) – when p markers are attached to $\mathscr{A}$ and q markers are attached to $\mathscr{B}$ – is *N-identifiable* if the set of non-identifying N-samples has measure 0 in $\mathcal{S}^N$. If there is no N such that (p, q) is N-identifiable, then the case (p, q) is said to be *non-identifiable* $\triangle$

The practical meaning of Definition 1 is clear. If the case (p, q) is *N-identifiable* then, given N random samples, *almost surely*, one can determine unambiguously the joint position and orientation in each frame. By contrast, if the case (p, q) is *non-identifiable*, then no matter how many samples we have at our disposal, we can never determine with certainty and unambiguously the position and orientation of the joint.

Remark 1 Clearly, if the case (p, q) is N-identifiable then so are the case (q, p) and the cases (p', q) for all $p' \geq p$. Similarly, if the case (p, q) is non-identifiable then so are the case (q, p) and the cases (p', q) for all $p' \leq p$ $\triangle$

Remark 2 Why identifiability can be achieved for only *almost all* and not for *all* N-samples? This is because of degenerate cases when the N-samples do not excite all the degrees of freedom of the joint. For a concrete example, see section IV-A $\triangle$

Note that the notion of identifiability studied in this article is not the same as the homonymous notion in control theory. The problem of joint parameters identification is formulated here in purely geometric terms and the actual identification – when possible – requires only a finite number of samples. On the other hand, this problem may also be formulated as the identification of the parameters of a *control system* if one uses the *continuous time series* of the positions of the markers. However, in such a formulation, one would need to take time derivatives, which would amplify the effect of measurement noise.

III. Identifiability results for revolute joints

A. The (2,1) case is 5-identifiable

To describe the position and orientation of the revolute joint axis – which is basically a line – in $\mathcal{F}$, we use the Denavit-Hartenberg convention (see Fig. 2, left). Following the notation convention of section II-A, one can note $\Pi_c = (d, r, \alpha)$, $\Pi_v = \theta$, $\Sigma_c = (l, \rho)$, $\Sigma_v = \beta$. The key here is to first obtain an equation relating Ω to the *constant* parameters Π_c, Σ_c, by eliminating the variable parameters Π_v and Σ_v.

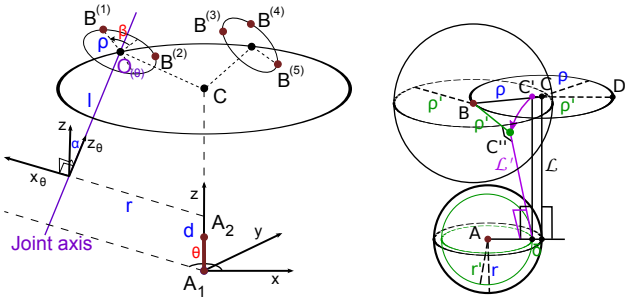

Fig. 2. **Left**: Revolute joint with two markers on one link (A_1, A_2 on $\mathscr{A}$) and one marker on the other link (B on $\mathscr{B}$). **Right**: Revolute joint with one marker on each link (A on $\mathscr{A}$ and B on $\mathscr{B}$).

1) Eliminating the variable parameters: The Denavit-Hartenberg matrix is given by

$$\mathbf{D} = \begin{pmatrix} \cos\theta & -\sin\theta\cos\alpha & \sin\theta\sin\alpha & r\cos\theta \\ \sin\theta & \cos\theta\cos\alpha & -\cos\theta\sin\alpha & r\sin\theta \\ 0 & \sin\alpha & \cos\alpha & d \\ 0 & 0 & 0 & 1 \end{pmatrix}.$$

Thus, the coordinates of O_θ in $\mathcal{F}$ is given by

$$\mathbf{D}\ (0,0,l,1)^\top = \begin{pmatrix} l\sin\theta\sin\alpha + r\cos\theta \\ -l\cos\theta\sin\alpha + r\sin\theta \\ l\cos\alpha + d \\ 1 \end{pmatrix}.$$

To eliminate the variable parameter β, remark that, a point (x,y,z) is on the circle of radius ρ, centered at O_θ, and orthogonal to the joint axis ($\mathbf{z}_\theta$) if and only if

$$\left\| \begin{matrix} x - l\sin\theta\sin\alpha - r\cos\theta \\ y + l\cos\theta\sin\alpha - r\sin\theta \\ z - l\cos\alpha - d \end{matrix} \right\|^2 = \rho^2, \tag{2}$$

and

$$\begin{pmatrix} x - l\sin\theta\sin\alpha - r\cos\theta \\ y + l\cos\theta\sin\alpha - r\sin\theta \\ z - l\cos\alpha - d \end{pmatrix}^\top \begin{pmatrix} \sin\theta\sin\alpha \\ -\cos\theta\sin\alpha \\ \cos\alpha \end{pmatrix} = 0. \tag{3}$$

Developing condition (3) yields

$$x\sin\theta - y\cos\theta = \frac{l + d\cos\alpha - z\cos\alpha}{\sin\alpha}. \tag{4}$$

Developing next condition (2) yields, after rearrangements,

$$x^2 + y^2 + z^2 + l^2 + r^2 + d^2 - \rho^2 +$$

$$2ld\cos\alpha - 2z(l\cos\alpha + d) - 2l\sin\alpha A - 2rB = 0,$$

where $A = x\sin\theta - y\cos\theta$ and $B = x\cos\theta + y\sin\theta$. Substituting A by the expression of equation (4) and regrouping terms then lead to

$$R^2 + Q - 2zd = 2rB, \tag{5}$$

where $R^2 = x^2 + y^2 + z^2$ and $Q = r^2 + d^2 - l^2 - \rho^2$. Remark next that, by the definitions of A and B, one has $A^2 + B^2 = x^2 + y^2$. Equation (5) is then equivalent to

$$R^2 + Q - 2zd = 2r\sqrt{x^2 + y^2 - \left(\frac{l + d\cos\alpha - z\cos\alpha}{\sin\alpha}\right)^2}. \tag{6}$$

Squaring the two sides of (6) and rearranging the terms then gives

$$(M_1 \dots M_5)(Y_1 \dots Y_5)^\top = K, \tag{7}$$

where

$$\begin{cases} M_1 &= -4R^2 z \\ M_2 &= 2R^2 \\ M_3 &= -4z \\ M_4 &= 1 \\ M_5 &= 4z^2 \end{cases} \tag{8}$$

$$\begin{cases} Y_1 &= d \\ Y_2 &= Q - 2r^2 \\ Y_3 &= Qd + \frac{2r^2\cos\alpha(l + d\cos\alpha)}{\sin^2\alpha} \\ Y_4 &= Q^2 + \frac{4r^2(l + d\cos\alpha)^2}{\sin^2\alpha} \\ Y_5 &= d^2 + \frac{r^2}{\sin^2\alpha} \end{cases} \tag{9}$$

and

$$K = -R^4.$$

Remark that, because of the squaring operation, equation (7) is a only a necessary (but not sufficient) condition for $\Omega = f(\Pi_c, \Pi_v, \Sigma_c, \Sigma_v)$. This point will be relevant later on.

2) Obtaining a linear system: Given now a 5-sample $\{(x^{(1)}, y^{(1)}, z^{(1)}), \dots, (x^{(5)}, y^{(5)}, z^{(5)})\}$, one can construct 5 equations similar to (7). Grouping these equations together, one obtains the matrix identity

$$\mathbf{MY} = \mathbf{K},$$

where $\mathbf{Y} = (Y_1 \dots Y_5)^\top$ and $\mathbf{M}$ and $\mathbf{K}$ are respectively a 5×5 matrix and a 5×1 vector constructed from the $x^{(1)}, y^{(1)}, z^{(1)}, \dots, x^{(5)}, y^{(5)}, z^{(5)}$.

Consider next the linear system of equations in the unknown $\mathbf{Z}$

$$\mathbf{MZ} = \mathbf{K}. \tag{10}$$

By construction, this equation has at least one solution $\widehat{\mathbf{Z}} = \mathbf{Y}$. This solution is *unique* if $\det(\mathbf{M}) \neq 0$.

3) The set of zeros of $\det(\mathbf{M})$*:* Developing $\det(\mathbf{M})$ and replacing the $R^{(i)}$ by their expressions in terms of $(x^{(i)}, y^{(i)}, z^{(i)})$ lead to

$$\det(\mathbf{M}) = P(x^{(1)}, y^{(1)}, z^{(1)}, \dots, x^{(5)}, y^{(5)}, z^{(5)}), \tag{11}$$

where P is a polynomial in 15 variables.

Let us have closer look at $\mathcal{S}$. By definition, $\mathcal{S}$ is the set of all (x,y,z) that satisfy equation (6). Solving equation (6) in z then gives z as an algebraic function (with possibly zero or multiple values) of x, y

$$z = g(x,y).$$

Replacing now $z^{(i)}$ by $g(x^{(i)}, y^{(i)})$ in (11) then gives the following identity

$$\det(\mathbf{M}) = h(x^{(1)}, y^{(1)}, \dots, x^{(5)}, y^{(5)}),$$

where h is an algebraic functions (with possibly zero or multiple values) in 10 variables. Furthermore, h is not the zero function (we have verified this by computing the value of h for a particular 5-sample). Therefore, by a well-known result on algebraic functions, the set of zeros of h has measure 0 in $\mathbb{R}^{10}$. As a consequence, the

set of $(x^{(1)}, y^{(1)}, z^{(1)}, \ldots, x^{(5)}, y^{(5)}, z^{(5)})$ in $\mathcal{S}^5$ such that $\det(\mathbf{M}) = 0$ also has measure 0.

4) Determining the joint parameters: Given now a 5-sample $\{(x^{(1)}, y^{(1)}, z^{(1)}), \ldots, (x^{(5)}, y^{(5)}, z^{(5)})\}$ such that $\det(\mathbf{M}) \neq 0$, one can solve system (10) to obtain a unique $\widehat{\mathbf{Z}}$. Letting $\widehat{\mathbf{Z}} = (Z_1, \ldots, Z_5)^T$, one has to solve the following systems to recover Π_c and Σ_c

$$\left\{\begin{array}{lcl} d & = & Z_1 \\ Q - 2r^2 & = & Z_2 \\ Qd + \frac{2r^2 \cos\alpha(l + d\cos\alpha)}{\sin^2\alpha} & = & Z_3 \\ Q^2 + \frac{4r^2(l+d\cos\alpha)^2}{\sin^2\alpha} & = & Z_4 \\ d^2 + \frac{r^2}{\sin^2\alpha} & = & Z_5 \end{array}\right. \tag{12}$$

The first equation of the system gives $d = Z_1$. Solving the remaining equations of the system by substitution leads to the following third-degree polynomial equation in Q

$$-Q^3 + aQ^2 + bQ + c = 0, \tag{13}$$

where $a = 2(Z_5 - Z_1^2) + Z_2 + 2Z_1^2$, $b = -4Z_1Z_3 + Z_4$, $c = 2Z_3^2 - Z_4(2(Z_5 - Z_1^2) + Z_2)$.

Equation (13) has 3 solutions (including possibly non-real solutions) Q_1, Q_2, Q_3. For each $k = 1, 2, 3$, one can next compute

$$\left\{\begin{array}{lcl} r_k & = & \sqrt{\frac{Q_k - Z_2}{2}} \\ \alpha_k & = & \operatorname{asin}\left(\sqrt{\frac{Q_k - Z_2}{2(Z_5 - d^2)}}\right) \\ l_k & = & \frac{Z_3 - Q_k d}{2(Z_5 - d^2)\cos\alpha_k} - d\cos\alpha_k \\ \rho_k & = & \sqrt{r_k^2 + d^2 - l_k^2 - Q_k}. \end{array}\right.$$

Remark that one of the Q_k corresponds to the extraneous solution added when squaring (5). This solution can be easily discarded by checking whether (5) is true for all samples. Next, a second Q_k is usually associated with non-real values for $r_k, \alpha_k, l_k, \rho_k$, and can also be discarded. Thus, there remains a unique Q_k, associated with unique values of r, α, l, ρ.

Finally, for each sample i, one can recover a unique $\theta^{(i)}$ by solving (4), and next a unique $\beta^{(i)}$ by a similar procedure.

B. The (1,1) case is non-identifiable

Here, Π_c consists of a single parameter r, which is the distance between the joint axis and the marker of $\mathscr{A}$ (see Fig. 2, right). Likewise, Σ_c consists of a single parameter ρ, the distance between the joint axis and the marker of $\mathscr{B}$.

Assume that we are given r, ρ, whose associated set of outputs is denoted $\mathcal{S}$. Our aim is to show that there exists r', ρ' with $r' \neq r$ such that $\mathcal{S}' \cap \mathcal{S}$ has measure > 0, where $\mathcal{S}'$ is the set of outputs associated with r', ρ'.

Consider indeed $r' = r - \delta$, $\rho' = \rho + \delta$ (for some small $\delta > 0$) and the set $\mathcal{S}_\Delta \subset \mathcal{S}$ consisting of samples whose distance from A is larger than some $\Delta > 0$. Note first that the measure of $\mathcal{S}_\Delta$ is > 0. Consider next an arbitrary sample $B \in \mathcal{S}_\Delta$ and a line $\mathcal{L}$ such that $\mathrm{d}(B, \mathcal{L}) = \rho$ and $\mathrm{d}(A, \mathcal{L}) = r$, where d denotes the distance between a line and a point. Such a line exists because $B \in \mathcal{S}$. Based on Fig. 2, one can construct another line $\mathcal{L}'$, such that $\mathrm{d}(B, \mathcal{L}') = \rho'$ and $\mathrm{d}(A, \mathcal{L}') = r'$, proving thereby that $B \in \mathcal{S}'$. Since B was chosen arbitrarily in $\mathcal{S}_\Delta$, one has $\mathcal{S}_\Delta \subset \mathcal{S}'$.

IV. Identifiability results for spherical joints

A. The (3,1) case is 4-identifiable

Here, since three markers are attached to link $\mathscr{A}$, it is fixed in the coordinate frame $\mathcal{F}$, and so is the joint center J. Thus, following the notation convention of section II-A, one has $\Pi_c = (x_J, y_J, z_J)$, $\Sigma_c = \rho$, $\Sigma_v = (\phi, \psi)$ (see Fig. 3, left).

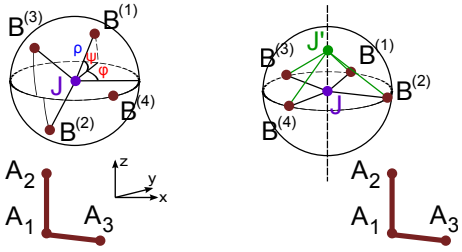

Fig. 3. Spherical joint with three markers on one link (A_1, A_2, A_3 on $\mathscr{A}$) and one marker on the other link (B on $\mathscr{B}$). **Left:** Non-degenerate 4-sample. Given any four non-coplanar samples $\{B^{(1)}, B^{(2)}, B^{(3)}, B^{(4)}\}$, the rotation center can be determined unambiguously. **Right:** A degeneracy arises when the samples are coplanar.

Remark that the set $\mathcal{S}$ of all possible outputs is actually a sphere of center J and of radius ρ. Given now 4 random samples $\{B^{(1)}, B^{(2)}, B^{(3)}, B^{(4)}\}$ (i.e. 4 random points on a fixed – but unknown – sphere), almost surely they are non-coplanar, and therefore, there exists a *unique* sphere that contains them. The center of this sphere, $J = (x_J, y_J, z_J)$, can be determined by computing the intersection of the mediating planes of $(B^{(1)}, B^{(2)})$, $(B^{(2)}, B^{(3)})$, and $(B^{(3)}, B^{(4)})$. The radius of this sphere, ρ, can next be determined by computing the distance between the center and any sample $B^{(i)}$. This establishes the 4-identifiability of the (3,1) case.

Degenerate cases A degeneracy arises when the 4 samples happen to be on the same plane (see Fig. 3, right). In such a case, any point J' belonging to the line perpendicular to this plane and going through J is equidistant from the samples and can thus play the role of a possible spherical joint. However, as remarked earlier, such a case occurs with probability 0 when the joint behaves as a real spherical joint, covering all the directions in space.

B. The (2,1) case is non-identifiable

As already detailed in section II-A, one has in this case $\Omega = (x, y, z)$, $\Pi_c = (d, r)$, $\Pi_v = \theta$, $\Sigma_c = \rho$, $\Sigma_v = (\phi, \psi)$ (see Fig. 1 and Fig. 4, left).

Assume that we are given d, r, ρ, whose associated set of outputs is denoted $\mathcal{S}$. As in section III-B, our aim here is to show that there exist r', ρ' with $r' \neq r$ such that $\mathcal{S}' \cap \mathcal{S}$ has measure > 0, where $\mathcal{S}'$ is the set of outputs associated with d, r', ρ'.

Denote by Γ the circle of radius r, perpendicular to the axis (A_1, A_2) and of z-coordinate d (see Fig. 4). Let r', ρ' be defined as follows: $r' = r - \delta$, $\rho' = \rho' + \delta$ for some small $\delta > 0$. Consider next an arbitrary $B \in \mathcal{S}$. By definition, there is a J on the circle Γ such that $\|BJ\| = \rho$. One can then show that the circle Γ', of radius r' and z-coordinate d, intersects

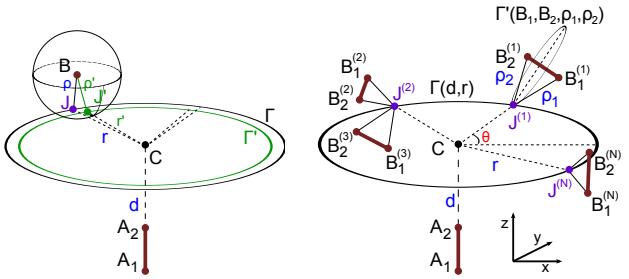

Fig. 4. **Left**: Spherical joint with two markers on one link (A_1, A_2 on $\mathscr{A}$) and one marker on the other link (B on $\mathscr{B}$). **Right**: Spherical joint with two markers on each link (A_1, A_2 on $\mathscr{A}$ and B_1, B_2 on $\mathscr{B}$)

the sphere of center B and radius ρ' at at least one point J'. This shows that $B \in \mathcal{S}'$, and since B was chosen arbitrarily in $\mathcal{S}$, one has $\mathcal{S} \cap \mathcal{S}' = \mathcal{S}$, which has measure > 0.

C. The (2,2) case is 9-identifiable

Following the notation convention of section II-A, one has here (see Fig. 4, right) $\Pi_c = (d, r)$, $\Pi_v = \theta$, $\Sigma_c = (\rho_1, \rho_2)$, $\Sigma_v = (\phi, \psi, \xi)$, where the three angles ϕ, ψ, ξ describe the orientation of the segment B_1B_2 around J.

Following the same line of reasoning as in section III-A, one first determines an equation relating d, r, ρ_1, ρ_2 and the outputs $B_1 = (x_1, y_1, z_1)$ and $B_2 = (x_2, y_2, z_2)$ as below

$$H^2(x_2^2+y_2^2)+G^2(x_1^2+y_1^2)-2HG(x_1x_2+y_1y_2)-r^2\delta^2 = 0, \quad (14)$$

where $\delta = x_1y_2 - x_2y_1$, and

$$\begin{cases} H = 1/2(x_1^2 + y_1^2 + (z_1 - d)^2 + r^2 - \rho_1^2) \\ G = 1/2(x_2^2 + y_2^2 + (z_2 - d)^2 + r^2 - \rho_2^2). \end{cases} \quad (15)$$

One can next transform equation (14) into a linear equation

$$(M_1 \dots M_9)(Y_1 \dots Y_9)^\top = K, \quad (16)$$

where $M_1, \dots, M_9, K$ are constructed from the $x_1, y_1, z_1, x_2, y_2, z_2$, and

$$\begin{cases} Y_1 = d^2 + r^2 - \rho_1^2 \\ Y_2 = d^2 + r^2 - \rho_2^2 \\ Y_3 = d \\ Y_4 = (d^2 + r^2 - \rho_1^2)(d^2 + r^2 - \rho_2^2) \\ Y_5 = (d^2 + r^2 - \rho_1^2)d \\ Y_6 = (d^2 + r^2 - \rho_2^2)d \\ Y_7 = (d^2 + r^2 - \rho_1^2)^2 \\ Y_8 = (d^2 + r^2 - \rho_2^2)^2 \\ Y_9 = r^2. \end{cases} \quad (17)$$

Finally, one can construct a linear system by grouping together 9 equations similar to (16) obtained from a 9-sample, and prove the 9-identifiability using the same arguments as in III-A.

V. Algorithms and Discussion

A. Identifying the hip joint using two markers per link

In sections III-A and IV-C, we have established the structural identifiability respectively in the (2,1) case for revolute joints and in the (2,2) case for spherical joints. Here we present practical algorithms to do such identifications in concrete settings.

We focus on the hip joint in humans, which can be modeled by a spherical joint linking the trunk and the thigh. A human subject performed a jumping motion from the floor onto a horizontal platform at ∼0.5m from the ground (see Fig. 5, right). Three markers were attached to the trunk: one on the fifth lumbar vertebra (L5: A_1), one on the left superior anterior iliac spine (LPELVIS: A_2) and one on the right superior anterior iliac spine (RPELVIS: A_3). Two markers were attached to the right thigh: one on the greater trochanter (RHIP: B_1) and one on the lateral epicondyle of the femur (RKNEE: B_2).

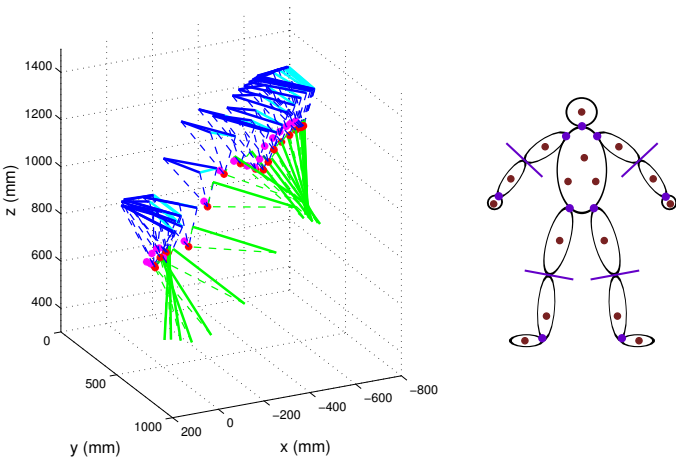

Fig. 5. **Left**: Identifying the hip joint position in a jumping motion (22 frames). Three markers were attached to the trunk (L5, LPELVIS, RPELVIS, forming the blue triangle, with the segment LPELVIS–RPELVIS in cyan) and two markers were attached to the thigh (RHIP and RKNEE, forming the green segment). For the Gamage-Lasenby method, all the 5 markers were used. The estimated joint position was plotted in red. For the new method we proposed, RPELVIS was excluded. The estimated joint position was plotted in magenta. **Right**: 16 markers are theoretically sufficient to identify all joints parameters in a 14-links, 31-dof, human model (the joints are depicted by violet dots and the markers by brown dots).

First, we extended the Gamage-Lasenby (GL) method [4, 2] to the case when both links are moving (the original GL algorithm assumes that one link is fixed in space). We used 22 frames taken every 95ms. In each frame i, we used the 3 trunk markers to compute an orthonormal reference frame $\mathcal{F}_i$ as follows: the origine of $\mathcal{F}_{\mathrm{GL}}^{(i)}$ was $A_1^{(i)}$; the first two vectors of the basis $(\mathbf{u}_1, \mathbf{u}_2)$ were obtained by orthonormalizing $\{A_2^{(i)} - A_1^{(i)}, A_3^{(i)} - A_1^{(i)}\}$; the third vector of the basis was defined by $\mathbf{u}_3 = \mathbf{u}_1 \times \mathbf{u}_2$. Because of non strict rigidity and measurement noise, the positions A_1, A_2, A_3 were not completely fixed in $\mathcal{F}_{\mathrm{GL}}^{(i)}$: instead, only A_1 was fixed, whereas A_2 and A_3 displayed some small variations. Next, we computed the coordinates of $B_1^{(i)}, B_2^{(i)}$ in $\mathcal{F}_{\mathrm{GL}}^{(i)}$ and gave these coordinates as input to the GL algorithm as described in [4]. This algorithm outputted the positions $J_{\mathrm{GL}}^{(i)}$ of the joint center in each frame.

We now describe a new algorithm [S22: Spherical joint, (2,2) case], which identifies the position of the joint center

using only *two* markers per rigid link: A_1, A_2, B_1, B_2. In each frame, we computed an orthonormal reference frame $\mathcal{F}_{\mathrm{S22}}^{(i)}$ as follows: the origine of $\mathcal{F}_{\mathrm{S22}}^{(i)}$ was still $A_1^{(i)}$; the first two vectors of the basis $(\mathbf{u}_1, \mathbf{u}_2)$ were obtained by orthonormalizing $\{A_2^{(i)} - A_1^{(i)}, \mathbf{v}\}$, where $\mathbf{v}$ is a random vector non-collinear with $A_2^{(i)} - A_1^{(i)}$; the third vector of the basis was still defined by $\mathbf{u}_3 = \mathbf{u}_1 \times \mathbf{u}_2$. Next, as in section IV-C, we place ourselves in the reference frame $\mathcal{F}_{\mathrm{S22}}^{(i)}$.

Remark that, if a tuple (d, r, ρ_1, ρ_2) is the correct answer and if there is no noise, the joint center would be given by the intersection of the circle $\Gamma(d, r)$ and $\Gamma'(B_1, B_2, \rho_1, \rho_2)$ (cf. section IV-C and Fig. 4, right). Following this remark, we computed, in each frame i, the point $J_{\mathrm{opt}}^{(i)}$ that minimized the sum $\mathrm{d}(J, \Gamma(d, r)) + \mathrm{d}(J, \Gamma'(B_1^{(i)}, B_2^{(i)}, \rho_1, \rho_2))$. Next, the cost associated with (d, r, ρ_1, ρ_2) was defined by

$$C(d, r, \rho_1, \rho_2) = \sum_{p=1,2} \mathrm{var}(\|J_{\mathrm{opt}} A_p\|) + \sum_{q=1,2} \mathrm{var}(\|J_{\mathrm{opt}} B_q\|),$$

where var is the variance computed across the frames. Note that the index p runs only from 1 to 2 because A_3 (RPELVIS) was excluded. Finally, we ran a global minimum search algorithm to find the optimal (d, r, ρ_1, ρ_2), which in turn is associated with a certain position $J_{\mathrm{S22}}^{(i)}$ of the joint center in each frame.

To assess the quality of this algorithm, we compare C_{S22} and C_{GL}, where the two measures were defined by

$$C_{\mathrm{S22}} = \sum_{p=1,2,3} \mathrm{var}(\|J_{\mathrm{S22}} A_p\|) + \sum_{q=1,2} \mathrm{var}(\|J_{\mathrm{S22}} B_q\|)$$

$$C_{\mathrm{GL}} = \sum_{p=1,2,3} \mathrm{var}(\|J_{\mathrm{GL}} A_p\|) + \sum_{q=1,2} \mathrm{var}(\|J_{\mathrm{GL}} B_q\|).$$

Note that the index p runs from 1 to 3 in both measures.

For the jumping motion of Fig. 5, we found that $\sqrt{C_{\mathrm{S22}}} = 9.18\mathrm{mm}$ and that $\sqrt{C_{\mathrm{GL}}} = 9.65\mathrm{mm}$, while the average distance across the frames between $J_{\mathrm{S22}}^{(i)}$ and $J_{\mathrm{GL}}^{(i)}$ was $43.26\mathrm{mm}$. In other words, our algorithm using only two markers on each link outperformed the extension of the GL method using three markers on one link and two markers on the other. Note however that there may exist better ways to extend the GL method to the case of two moving links (based e.g. on [5]). Also, the GL method gives a closed-form solution while our method must rely on an iterative minimum search (the closed-form solution given by the formulae of section IV-C is too sensitive to noise and non strict rigidity). We are currently trying to find a robust closed-form solution based on the formulae of section IV-C.

In contrast with the optimization technique of [6], which uses a distance penalty unrelated to the problem at hand and solely intended to guarantee the convergence of the algorithm to sensible values, our method involves no such extra, arbitrary, constraint. Furthermore, the issue of local minima is considerably alleviated since the dimension of our optimization problem is 4 (d, r, ρ_1, ρ_2), which is much smaller than that in [6], which is $3N$, where N is the number of frames.

B. Joint parameter identification in full-body motion capture

Using the results just established, it is theoretically possible to identify all joint parameters in a 14-links, 31-dof, human model using just 16 markers as illustrated in Fig. 5, right panel.

One starts with 3 markers on the trunk, which allow determining completely the position and orientation of the trunk in space. Next, using the marker on the thigh, one can identify the position of the hip joint [spherical joint, (3,1) case]. The position of the hip joint together with the thigh marker thus provides two "markers" on the thigh. Next, using these two "markers" and the shank marker, one can identify the parameters of the knee joint [revolute joint, (2,1) case]. The position and orientation of the knee joint in turn gives the full position and orientation of the thigh and the shank. Finally, the parameters of the ankle joint can be determined using the shank full position and orientation together with the foot marker [spherical joint, (3,1) case]. The same procedure can be repeated for the remaining leg and the two arms. The neck joint parameters can finally be identified using the trunks markers and the head marker [spherical joint, (3,1) case].

C. Conclusion

We have studied the minimum number of markers that are necessary to identify the parameters of revolute and spherical joints and have presented a practical algorithm to do the identification in the case of a spherical joint with two markers attached to each of the adjacent link. Our current research focuses on the implementation of the identification of joint parameters using a minimum number of markers in a full-body setting.

Acknowledgments

This research was funded in part by a JSPS postdoctoral fellowship awarded to the first author and by a Grant-in-Aid of Category S for Scientific Research (20220001) of the JSPS.

REFERENCES

[1] R. Bellman and KJ Astrom. On structural identifiability. *Mathematical Biosciences*, 7(3-4):329–339, 1970.

[2] R.M. Ehrig, W.R. Taylor, G.N. Duda, and M.O. Heller. A survey of formal methods for determining the centre of rotation of ball joints. *Journal of Biomechanics*, 39(15):2798–2809, 2006.

[3] R.M. Ehrig, W.R. Taylor, G.N. Duda, and M.O. Heller. A survey of formal methods for determining functional joint axes. *Journal of Biomechanics*, 40(10):2150–2157, 2007.

[4] S.S. Gamage and J. Lasenby. New least squares solutions for estimating the average centre of rotation and the axis of rotation. *Journal of Biomechanics*, 35(1):87–93, 2002.

[5] B.K.P. Horn. Closed-form solution of absolute orientation using unit quaternions. *J. Opt. Soc. Amer. A*, 4(4):629–642, 1987.

[6] A.G. Kirk, J.F. O'Brien, and D.A. Forsyth. Skeletal parameter estimation from optical motion capture data. In *IEEE Conference on Computer Vision and Pattern Recognition*, pages 782–788, 2005.

[7] Y. Nakamura, K. Yamane, Y. Fujita, and I. Suzuki. Somatosensory computation for man-machine interface from motion-capture data and musculoskeletal human model. *IEEE Transactions on Robotics*, 21(1):58–66, 2005.

[8] K. Yamane and Y. Nakamura. Dynamics filter – concept and implementation of online motion generator for human figures. *IEEE Transactions on Robotics and Automation*, 19(3):421–432, 2003.